Available online at www.scholarsresearchlibrary.com

Scholars Research Library

J. Nat. Prod. Plant Resour., 2015, 5 (2): 20-32
(http://scholarsresearchlibrary.com/archive.html)

ISSN : 2231 – 3184
CODEN (USA): JNPPB7

A Comparative Study of the Inhibitory Action of the Extracts of *Garcinia indica*Choisy, *Terminalia chebula*Retz.and*Coriandrumsativum*L. on the Corrosion of Aluminum and 6063 Aluminum alloy in Sodium Hydroxide Medium

Deepa Prabhu[1] and Padmalatha[2*]

[1]International Center for Applied Sciences, Manipal University, Karnataka, India
[2]Department of Chemistry, Manipal Institute of Technology, Manipal University, Karnataka, India

---

ABSTRACT

Plant extracts of Garcinia indicaChoisy, Terminalia chebulaRetz.andCoriandrumsativumL.were investigated for their efficiency in inhibiting the corrosion of aluminum and 6063 aluminum alloy in sodium hydroxide medium. The techniques like weight loss and potentiodynamic polarizationwere employed. The inhibition was proposed to be the result of adsorption of constituents of extract, which was found to obey the Langmuir adsorption isotherm. The inhibition was assumed to be the formation of a protective inhibitor layer formed on the surface of material.

Keywords: aluminum, 6063 aluminum alloy, sodium hydroxide, *Garcinia indica*Choisy, *Terminalia chebula*Retz., *Coriandrumsativum*L., weight loss, potentiodynamic polarization

---

INTRODUCTION

Aluminum has a wide range applications especially in aerospace, household industry and is commonly used in marine applications. This is because of the combination of unique properties like light weight, good appearance, high mechanical strength, thermal and electrical conductivity.Pure aluminum is soft and has low tensile strength, and most of the time alloyed with other metals. The typical alloying elements of aluminum are copper, magnesium, manganese, silicon and zinc. Aluminum alloys with a wide range of properties are used in engineering structures, like aircrafts due to their high strength-to-weight ratio [1].

Sodium hydroxide is used for alkaline cleaning, pickling and etching of aluminum and aluminum alloys [1]. It is widely used for degreasing equipment used in the food industry. Acidic or alkaline pickling treatments generally applied at the beginning of surface treatments. Inhibitors are generally used to minimize the attack of the metal by acids or alkalis present in the pickling bath.

Now-a-days environmental issues related to the use of some organic compounds have received global attention.Plant products are emerging as inexpensive, eco-friendly corrosion inhibitors and gaining rapt attention of many researchers [2, 3].

MATERIALS AND METHODS

2.1 Materials and preparation of test coupons

The experiments were carried out with test coupons (specimens) of aluminum and 6063 aluminum alloy. The compositions of both the materials are given in Table 1. Cylindrical test coupons were cut from the rods and sealed with epoxy resin. The areas of the metal exposed to the corrosive were 0.7 cm^2 for aluminum and 1.0 cm^2 for 6063 aluminum alloy. These test coupons were first polished by emery papers of different grades (in the range of 600-2000) and then followed by legated alumina paste. The polished test coupons were washed with double distilled water,degreased with acetone and thoroughly dried before immersing into the corrosive.

2.2 Preparation of medium

Sodium hydroxide (Merck, Analar Grade) and double distilled water were used for the preparation of medium. The sodium hydroxide was standardized by volumetric method, by titrating it with standard potassium hydrogen phthalate using phenolphthalein indicator. Sodium hydroxide solutions each of required concentrations (0.5 M, 1.0 M, 2.0 M) were prepared freshly as and when required by appropriate dilution of standardized stock solutions.
Experiments were performed using calibrated thermostat at temperatures 30 ℃, 35 ℃, 40 ℃, 45 ℃, 50 ℃ (±0.5 ℃) under unstirred conditions.

2.3 Preparation of inhibitors

2.3.1 Selection of plants and authentication

While selecting the plant materials, maximum importance was given for availability of plants in the local area, ease of identification, non- toxicity and the cost. Literature survey revealed that *Garcinia indica*Choisy, *Terminalia chebula*Retz.and*Coriandrumsativum*L. were not used as inhibitors for corrosion control of aluminum and 6063 aluminum alloy in phosphoric acid and sodium hydroxide medium. Selected plants and the seeds were authenticated by Botanist, Prof. V. AravindaHebbar, former H.O.D, Department of Botany, Bhandarkar's college, Kundapura, Karnataka.

2.3.2 Plant profile

(i) *Garcinia indica*Choisy

*Garcinia indica*Choisy(kokum)belongs to the botanical family Clusiaceae also known as Guttiferae.The genus *Garcinia* contains 200 species out of which over 20 arefound in India. Kokum is an evergreen tree predominantly grown in the tropical humid rainforests ofWestern Ghats in South India up to an elevation of around 800 meters.*Garcinia indica*Choisyaqueousextract, contains large amount of polyisoprenylatedbenzophenone derivatives such as Garcinol and its colorless isomer, Isogarcinol. In addition to this, fruits of *Garcinia indica*Choisy reported to contain small amount of malic acid, polyphenols, carbohydrates, anthocyanin, pigments and ascorbic acid [4].

(ii) *Terminalia Chebula*Retz.

Terminalia chebula Retz. (Sanskrith: Haritaki, Kannada: Alalekaayi) tree belongs to the genus *Terminalia*, family Combretaceae. The dried ripe fruits of *Terminalia chebula* Retz are extensively used in ayurvedicamedicine because of their homeostatic, laxative, diuretic, cardiotonic and antioxident activities [5]. Principal active constituents of fruits of *Terminalia chebula*Retz.are tannins up to 30 %, chebulic acid 3-5 %, chebulinic acid 30 %, tannic acid 20-40 %, ellagic acid, 2,4-chebulyi–β-D-glucopyranose, gallic acid, ethyl gallate, etc. [6].

(iii) *Coriandrumsativum*L.

Coriandrumsativum L. (Coriander) is a medicinal and culinary plant from the Apiaceae (also known as Umbelliferae) family [7]. Coriander seed extract exhibits antibacterial, antioxidant, anticancer and antimutagenic activities. Major component of aqueous extract of coriander seeds consists of essential oils (0.2-1.0 %). The essential oil mainly contains linalool (60-70 %), α-pinene (10 %), γ-terpinene (9 %), geranyl acetate (4%) [8].

2.3.3 Preparation of aqueous extract of inhibitors

Seeds of *Garcinia indica*Choisy, *Coriandrumsativum* L. and fruits of *Terminalia chebula* Retz. were collected and dried [9]. Dried seeds were grinded well. 10 g of powdered sample was refluxed with 100 mL of distilled water for 3 h. The refluxed solution was kept overnight and then filtered carefully. Filtratewas heated slowly on a water bath to remove water contents. After the evaporation dry brown powder was obtained.

2.4 Weight loss method

Weight loss method was adopted to study the corrosion inhibition of green inhibitor in sodium hydroxide medium. The experiment was carried out at 30 ℃, by varying the concentrations of medium and inhibitors. The experimental solution was 100 mL of different concentrations of sodium hydroxide in absence and presence of different concentrations of inhibitors. The initial weight of the test coupon was noted and then it was completely immersed into the experimental solution for 2 h. After 2 h, the test coupon was taken out, washed thoroughly with distilled water, dried and their final weight was noted to the nearest 0.0001 g using a digital analytical balance (citizen CY 204). From the initial and final weights of the test coupons, the loss in weight was calculated.

2.5Potentiodynamic polarization (PDP) measurements

An electrochemical work station, (CH600D-series, U.S. Model with CH instrument beta software) was used to perform electrochemical measurements. A conventional three-electrode compartment Pyrex glass cell assembly was used to conduct electrochemical measurements [10, 11]. The working electrode was aluminum or 6063 aluminum alloy specimens. A rectangular platinum foil was used as an auxiliary electrode to exert uniform potential on the working electrode. Saturated calomel electrode (SCE) was used as a reference electrode. Finely polished test coupons were exposed to sodium hydroxide solution of known concentration, without and with inhibitors of different concentrations at different temperatures (30 ℃ to 50 ℃) and allowed to establish a steady-state open circuit potential (OCP) for about 30 minutes. Test coupons were then polarized by the application of potential drift of −250 mV cathodically and +250 mV anodically with respect to the OCP at a scan rate of 1.0 mVs^{-1}. The potentiodynamic polarization plots (Tafel curves) were developed simultaneously.

In all the studies, minimum of 3-4 trails were done and average of best three agreeing values was reported.

2.6 Effect of temperature and evaluation of kinetic parameters

The corrosion rates determined at various temperatures (30 ℃ - 50 ℃) by the potentiodynamic polarization method were used for the determination of energy of activation (E_a), enthalpy of activation ($\Delta H^{\#}$) and entropy of activation ($\Delta S^{\#}$).Energy of activation (E_a) was calculated from the Arrhenius equation [12]. Enthalpy of activation ($\Delta H^{\#}$) and entropy of activation ($\Delta S^{\#}$) were calculated using transition state equation [12].

2.7 Adsorption isotherms and determination of thermodynamic parameters

The adsorption of organic molecules takes place at the metal-solution interface. Adsorption of inhibitors depends mainly on the charge acquired by metal surface, electronic characteristics of metal surface, adsorption of solvent and other ionic species, temperature of corrosive and on the electrochemical potential at solution-interface [13, 14].
Adsorption isotherm is usually used to describe the interaction between the inhibitor molecule and metal surface. An adsorption isotherm is a graphical representation relating extent of adsorption in terms of surface coverage(θ), with concentrations of adsorbate at a constant temperature [13].

Different types of adsorption isotherm which are tried to fit in the experimental data [15]. The correlation coefficient (R^2) was used to choose the isotherm that best fit experimental data. From the adsorption equilibrium constant (K), standard free energy of adsorption (ΔG^{o}_{ads}) was calculated [16]. Other thermodynamic parameters like standard enthalpy of adsorption ($\Delta H°_{ads}$) and standard entropy of adsorption ($\Delta S°_{ads}$) were obtained by plotting graph of standard free energy of adsorption ($\Delta G°_{ads}$)versustemperature.

RESULTS AND DISCUSSION

3.1 Weight loss measurements

Weight loss measurements were done by studying the influence of concentrations of GIE, TCE and CSE on the corrosion of aluminum and 6063 aluminum alloy at 30 ℃ for a period of 2 h. The variation of inhibition efficiency of inhibitors for the corrosion of aluminum and 6063 aluminum alloy in different concentrations of sodium hydroxide containing different concentrations ofCSEat 30℃ is shown in Figure 1. Similar behavior is observed for GIE and CSE.Results of weight loss measurements for the corrosion of aluminum and 6063 aluminum alloy in sodium hydroxide containing different concentrations of inhibitors at 30 ℃ is given in Table 2.
As the concentrations of the inhibitor increased, weight loss of aluminum decreased, and the inhibition efficiency increased. Beyond the optimum concentration, there was no improvement in the inhibition efficiency, indicating the optimum concentration of the inhibitor to get maximum corrosion inhibition.

3.2 Potentiodynamic polarization (PDP) measurements

The potentiodynamic polarization measurements for the corrosion of aluminum and 6063 aluminum alloy specimen were carried out in different concentrations sodium hydroxide (0.5 M, 1.0 M and 2.0 M) containing different concentrations of GIE, TCE and CSE (0.05-0.6 g L^{-1}) at different temperatures (30-50 ℃). Figure 2 depicts the potentiodynamic polarization plots for the corrosion of aluminum and 6063 aluminum alloy in 0.5 M sodium hydroxide containing different concentrations of CSE at 30 ℃. Similar plots were obtained for other two concentrations of sodium hydroxide at four different temperatures and also for other inhibitors studied. The maximum inhibition efficiency reported corresponds to the optimum concentration of the inhibitor. Results of potentiodynamic polarization measurements for the corrosion of aluminum and 6063 aluminum alloy in 0.5 M sodium hydroxide containing different concentrations of inhibitors at 30 ℃ is given in Table 3.

The corrosion rate (*CR*) was calculated using equation (1) [17].

$$CR\left(\text{mm y}^{-1}\right) = \frac{K \text{ x } M \text{ x } i_{corr}}{\rho \text{ x } Z} \quad (1)$$

where K = 3.27 mm g/mA cm y, and it defines the unit of corrosion rate (in mm y^{-1}), i_{corr} is the corrosion current density (in mA cm^{-2}), ρ is the density of the corroding material (in g cm^{-3}), M is the atomic mass of the metal, and Z is the number of electrons transferred per atom. For aluminum and aluminum alloys M = 27, ρ = 2.7 g cm^{-3} and Z = 3. Using equation (2) the percentage inhibition efficiency (*IE* %) was calculated.

$$IE(\%) = \theta \times 100 \quad (2)$$

where;

$$\theta = \frac{i_{corr} - i_{corr(inh)}}{i_{corr}} \quad (3)$$

wherei_{corr} and $i_{corr(inh)}$are the corrosion current densities obtained for uninhibited and inhibited solutions respectively. Results of the potentiodynamic polarization measurements indicated decrease in corrosion current density (i_{corr}) after the addition of the inhibitor. The inhibition efficiency increased with the increase in concentrations of all the three inhibitors, up to an optimum value. Thereafter the increase in the inhibitor concentration resulted in negligible increase in the inhibition efficiency. There was no significant change in the values of cathodicTafel slope (β_c) and anodic Tafel slope (β_a) with inhibitor concentrations[18]. This indicates that the addition of the inhibitor does not change the hydrogen evolution reaction mechanism [19] and its non−interference in the mechanism of anodic reaction [20, 21].

Appreciable shift in the corrosion potential (E_{corr}) was not observed after the addition of inhibitors to the corrosion medium and also after increasing its concentration. Available literature indicates that [20], if the shift in corrosion potential is more than ±85 mV with respect to that of the blank, then the inhibitor can be considered either as a cathodic or anodic type. However, the maximum displacement in the present investigation was less than ±85 mV, with a shift towards the anodic side. This indicates that all the studied inhibitors acts as a mixed type of inhibitor with a major control over anodic reaction of metal dissolution. The inhibition efficiency increased with the increase in concentration of inhibitors, supporting increase in surface coverage. These observations and discussions are applicable both for aluminum and 6063 aluminum alloy.

3.3 Effect of temperature and kinetic parameters

The effect of temperature on the corrosion of aluminum and 6063 aluminum alloy was studied by measuring the corrosion rate at different temperatures between 30−50 ℃. The corrosion rate increased with increase in temperature. This observation could be related to the fact that, as the temperature increases the naturally occurring oxide film becomes thin, porous and less protective. The increase in the inhibition efficiency of GIEwith increase in temperature indicate that adsorption of GIE may be chemisorption. The decrease in the inhibition efficiency of TCE and CSE with increase in temperature provides a clue that mechanism of adsorption may be physisorption. Physical adsorption is mainly because of electrostatic interaction and electrostatic force of attraction decreases with increase in temperature.

Energy of activation (E_a) was calculated from the Arrhenius equation (4):

$$\ln(CR) = B - \frac{E_a}{RT} \quad (4)$$

where$B$ is a constant which varies from one metal type to another, R is the universal gas constant (8.314 J mol^{-1} K^{-1}), and T is the absolute temperature. Arrhenius plots in 0.5 M sodium hydroxide containing different concentrations of CSE for the corrosion of aluminum and 6063 aluminum alloy is given in Figure 3. Similar plots are obtained for GIE and CSE.

The enthalpy of activation ($\Delta H^{\#}$) and entropy of activation ($\Delta S^{\#}$) were calculated using transition state equation (5):

$$\mathrm{CR} = \frac{RT}{Nh} \exp\left(\frac{\Delta S^{\#}}{R}\right) \exp\left(\frac{\Delta H^{\#}}{RT}\right) \quad (5)$$

where$h$ is Plank's constant (6.626×10^{-34} J.s), N is Avogadro's number (6.022×10^{23} mol^{-1}) and T is the absolute temperature. Plots of ln (CR/T) versus ($1/T$) gave straight lines. Enthalpy of activation ($\Delta H^{\#}$) was deduced from the slope (slope = $-\Delta H^{\#}/\mathrm{R}$) and entropy of activation ($\Delta S^{\#}$) was evaluated from the intercept (intercept = $\ln(R/Nh) + \Delta S^{\#}/\mathrm{R}$).Plots of ln ($CR/T$) versus $1/T$ in 0.5 M sodium hydroxide containing different concentrations of CSE for the corrosion of aluminum and 6063 aluminum alloy is given in Figure 4. Similar plots are obtained for GIE and CSE. Activation parameters for the corrosion of aluminum and 6063 aluminum alloy in 0.5 M sodium hydroxide containing different concentrations of inhibitors is given in Table 4.

The energy of activation (E_a) for GIE was lower than that of blank solution. With increase in concentrations of GIE, the energy of activation decreased. It is an indication of chemisorption [22, 23]. With increase in the concentration of TCE and CSE energy of activation (E_a) increased. It indicates increase in energy barrier for the corrosion reaction. The extent of increase was proportional to the inhibitor concentrations. It indicates that the energy barrier for the corrosion reaction increased with increase in TCE and CSE concentrations.

The activation enthalpy ($\Delta H^{\#}$) varied in the same manner as the activation energy (E_a), supporting the proposed inhibition mechanism. The entropy of activation ($\Delta S^{\#}$) in the absence and presence of the inhibitor were large and negative indicating that the activated complex represents association rather than dissociation step [24].

3.4 Adsorption isotherms and thermodynamic parameters

The interaction between inhibitor molecules and the metal surface can be understood by adsorption isotherms. From the potentiodynamic polarization measurements, the degree of surface coverage (θ) for different concentrations of inhibitor was evaluated. The data were tried to fit into different adsorption isotherms. The Langmuir, Freundlich, Temkin, Frumkin and Flory–Huggins were the important adsorption isotherms considered to fit the experimental data. The best fit was achieved with the Langmuir adsorption isotherm.

The Langmuir adsorption isotherm mathematically can be represented by following equation (6):

$$\frac{C_{inh}}{\theta} = C_{inh} + \frac{1}{K} \quad (6)$$

where$K$ is the adsorption equilibrium constant, C_{inh} is inhibitor concentrations (in g L^{-1}) and θ is the surface coverage.Langmuir adsorption isotherms for the adsorption of CSE in 0.5 M sodium hydroxide at different temperatures for the corrosion of aluminum and 6063 aluminum alloy is given in Figure 5. Similar plots are obtained for GIE and CSE.

From the adsorption equilibrium constant (K), standard free energy of adsorption ($\Delta G°_{ads}$) can be calculated using the equation (7):

$$\Delta G°_{ads} = -RT \ln K \quad (7)$$

where*R* is the universal gas constant (8.314 J mol^{-1} K^{-1}), *T* is the absolute temperature. It is well known that the unit for $\Delta G°_{ads}$is J mol^{-1}. Since the unit for the term *RT*is also J mol^{-1}, adsorption equilibrium constant (*K*)in Eq. (3.9) must be dimensionless [16].

However, by taking the units of concentration of inhibitor and water same, *K* obtained from the equation 4.11 will be in the dimension of L $g^{-1.}$ In such a situation, *K* can be easily recalculated as dimensionless by multiplying it by 1000 (number of grams of water per liter of solution) [25]. Accordingly, the correct $\Delta G°_{ads}$value can be obtained from the equation (8):

$$\Delta G°_{ads} = -RT \ln(1000K) \quad (8)$$

The valuable information regarding the mechanism of the corrosion inhibition can be obtained from thermodynamic parameters. Standard enthalpy of adsorption ($\Delta H°_{ads}$) and standard entropy of adsorption ($\Delta S°_{ads}$) can be calculated from equation (9):

$$\Delta G°_{ads} = \Delta H°_{ads} - T\Delta S°_{ads} \quad (9)$$

A plot of $\Delta G°_{ads}$versus temperature gave straight line, with a slope (slope = $-\Delta S°_{ads}$) and an intercept (intercept = $\Delta H°_{ads}$). Plot of free energy of adsorption versus temperature for the adsorption of CSEin 0.5 M sodium hydroxide for the corrosion ofaluminum and 6063 aluminum alloy is given in Figure 6. Similar plots are obtained for GIE and CSE. Thermodynamic parameters for the adsorption of inhibitors on aluminum and 6063 aluminum alloy in 0.5 M sodium hydroxide at different temperatures is given in Table 5.

With GIE as inhibitor, the standard free energy of adsorption ($\Delta G°_{ads}$) was more than -20 kJ mol^{-1} at all studied concentrations of sodium hydroxide at all temperatures. The standard free energy of adsorption ($\Delta G°_{ads}$) decreased with increase in temperature. These two observations suggests chemical adsorption of the inhibitor on surface of the metal [22].

As per the reported literature, chemisorption is observed during the endothermic process where, the enthalpy of adsorption is positive ($\Delta H°_{ads} > 0$) [26]. An exothermic adsorption process with the negative value of enthalpy of adsorption ($\Delta H°_{ads} < 0$) may involve either physisorption or chemisorption or a mixture of both processes [27]. In the present investigation, with GIE as inhibitor, the positive value of the enthalpy of adsorption ($\Delta H°_{ads}$) proves beyond ambiguity that adsorption of GIE proceeds by chemisorption. Increase in the inhibition efficiency of GIE with increase in temperature also complements the suggested chemisorption mechanism for the adsorption of GIE on aluminum and 6063 aluminum alloy.

Standard free energy of adsorption ($\Delta G°_{ads}$) for TCE and CSEwere around -20 kJ mol^{-1} and it increased with the increase in temperature. This is an indication of physical adsorption of TCE and CSE on the surface of aluminum and 6063 aluminum alloy [28, 29]. Enthalpy of adsorption ($\Delta H°_{ads}$) was negative. The negative value of enthalpy of adsorption ($\Delta H°_{ads}$) is characteristics of exothermic process, which further confirms physisorption of TCE and CSE molecules on surface of the metal[28].

The value of standard entropy of adsorption ($\Delta S°_{ads}$) was large and negative. This is an indication of adsorption of inhibitors, which is accompanied by a reduction in entropy. Before the adsorption of components of the extracts onto the aluminum surface, components of the extracts might freely move in bulk of solution, but with the progress in the adsorption, components of the extracts were orderly adsorbed onto the aluminum surface, resulting in a decrease in entropy [30-32].

3.5 Mechanism of corrosion and inhibition process

Corrosion of metals is known to proceed by the action of local cells, which are established by metals, comprising a partial anodic and cathodic reaction occurring simultaneously on the surface of metal [10, 33]. In order to understand the mechanism underlying the corrosion of metals, it is necessary to explore which partial anodic and cathodic reactions involved during corrosion. Dissolution of aluminum in alkali, can be expressed by following anodic and cathodic processes [34].

Inhibitor molecules get adsorbed on surface of the metal, via physisorption or chemisorption. Following are the different modes through which either of the two adsorption process take place:

(i) Chemisorption, which involves sharing of electrons between heteroatoms of neutral inhibitor molecule and the metal surface
(ii) Physisorption, which involves the adsorption of positively/ negatively charged part of the inhibitor molecules on negatively/positively charged aluminum surface [35].
Inhibitor molecules must displace water molecules which are already adsorbed on the surface of the metal. It can be represented by equation (10).

$$\text{Inhibitor}_{(sol)} + \times H_2O_{(ads)} \rightleftharpoons \text{Inhibitor}_{(ads)} + \times H_2O_{(sol)} \quad (10)$$

Evaluation of the activation parameters of GIE indicated decrease in the energy of activation (E_a) of inhibited solution compared to that of blank solution. This observation is an indication of chemical adsorption of the inhibitor on the surface of the metal. Further, positive value of standard enthalpy of adsorption ($\Delta H°_{ads}$) for GIE complements the possibility of chemisorption of the inhibitor molecules on the surface of aluminum and 6063 aluminum alloy. Chemisorption arises from the donor- acceptor interaction between metal and the inhibitor molecules having heteroatoms, π electrons of multiple bonds as well as phenyl groups and vacant p orbitals of the metal.

pH dependent surface charge on surface of aluminum is due to the interaction of terminal oxygen atoms of aluminum oxide surface with water resulting in the formation of hydroxylated sites, or hydroxide layers at the surface (M–OH). At higher pH, a hydroxide surface loses protons to produce the negatively charged metal surface ($Al–O^-$) (equation 11).

$$Al - OH + OH^- \rightarrow Al - O^- + H_2O \quad (11)$$

In other words surface of aluminum is negatively charged in alkaline environment [34, 36]. Positively charged sodium ions will be electrostatically attracted by aluminum surface and gets physically adsorbed on it. [19, 37].

The inhibition effect of TCE and CSE are attributed to the presence of organic compounds present in the extract [38]. Phenolic –OH groups are acidic in nature. In the presence of alkali, they get deprotonated [39]. The deprotonated molecules of the inhibitor get physically adsorbed over the positively charged metal surface, in accordance with the equation (12):

$$\mathbf{Al}\text{-}O^- \rightarrow \mathbf{Al}\text{-}O^{-}\text{--}Na^+_{(ads)} \rightarrow \mathbf{Al}\text{-}O^{-}\text{--}Na^+_{(ads)}\text{--}(Inh)^-_{(ads)} \quad (12)$$

Overall, consequence of the adsorption of inhibitor molecules is the formation of protective layer on surface of the aluminum. This will form a barrier between the metal and corrosive and prevent further dissolution of the metal [25]. Consequently there was substantial decrease in the rate of corrosion.

In alkaline aqueous solution, a fraction of principal active constituents of TCE and CSE may exist in the deprotonated form and remaining as neutral molecules. These deprotonated –OH groups of the inhibitor molecules can get physically adsorbed on the positively charged sites and brings anodic reaction under control. The higher inhibition efficiency was observed for TCE than CSE due to the large size of the active constituents, which exert umbrella effect. The inhibitor molecule is large enough to cover both anodic and cathoidic area. As a result of this, both anodic and cathodic reactions come under control. Hence it acts as a mixed type of inhibitor, with more control over the anodic reaction.

3.6Effect of concentration of sodium hydroxide medium
It was evident from both weight loss method and potentiodynamic polarization method that, with increase in concentrations of sodium hydroxide, there was increase in the corrosion rate and decrease in the inhibition efficiency. The decreased inhibition efficiency in at higher concentrations of sodium hydroxide can be attributed to the higher corrosively of the medium [40]. The present investigation also aims to find the optimum concentration of

the inhibitor required to get the maximum inhibition efficiency. Hence different concentrations of the inhibitor were tried in different concentrations of sodium hydroxide. These values are tabulated in Table 6.

Table 1: Composition of the aluminum and 6063 aluminum alloy specimen

Element	Composition (weight %)	
	Aluminum	6063 aluminum alloy
Si	0.120	0.412
Fe	0.270	0.118
Cu	−	0.0570
Mg	−	0.492
Al	Balance	Balance

Table 2: Results of weight loss measurements for the corrosion of aluminum and 6063 aluminum alloy in sodium hydroxide containing different concentrations of inhibitors at 30 ℃

Inhibitor	Aluminum			6063 Aluminum alloy	
	Conc. of inhibitor ($g\ L^{-1}$)	Weight loss (mg)	*IE* (%)	Weight loss (mg)	*IE* (%)
GIE	Blank	101.2	−	129.8	−
	0.05	66.65	34.14	74.57	42.55
	0.1	62.57	38.17	66.67	48.64
	0.2	57.69	42.99	60.53	53.37
	0.3	51.93	48.69	56.71	56.31
	0.4	48.21	52.36	48.39	62.72
TCE	Blank	101.2	−	129.8	−
	0.05	52.34	48.28	56.36	56.58
	0.1	45.58	54.96	48.92	62.31
	0.2	41.08	59.41	43.73	66.31
	0.3	36.95	63.49	37.24	71.31
	0.4	31.21	69.16	31.79	75.51
CSE	Blank	101.2	−	129.8	−
	0.1	70.85	29.99	84.12	35.19
	0.2	62.11	38.63	73.04	43.73
	0.3	56.12	44.55	64.58	50.25
	0.4	43.82	56.70	48.68	62.50
	0.5	36.08	64.35	38.62	70.25

Table 3: Results of potentiodynamic polarization measurements for the corrosion of aluminum and 6063 aluminum alloy in 0.5 M sodium hydroxide containing different concentrations of inhibitors at 30 ℃

Inhibitor	Aluminum						6063 Aluminum alloy				
	Con. of inhibitor ($g\ L^{-1}$)	E_{corr} (mV vs SCE)	i_{corr} (m A cm^{-2})	β_a (m V dec^{-1})	$-\beta_c$ (m V dec^{-1})	*IE* (%)	E_{corr} (mV vs SCE)	i_{corr} (m A cm^{-2})	β_a (m V dec^{-1})	$-\beta_c$ (mV dec^{-1})	IE (%)
GIE	Blank	−1567	2.50	510	474	−	−1560	3.26	485	472	−
	0.05	−1583	1.57	490	493	37.09	−1542	1.78	493	501	45.33
	0.1	−1585	1.47	467	506	41.12	−1548	1.60	495	486	50.78
	0.2	−1589	1.35	469	479	45.94	−1551	1.46	494	478	55.14
	0.3	−1595	1.21	485	512	51.64	−1553	1.32	505	468	59.56
	0.4	−1599	1.12	479	494	55.31	−1555	1.15	501	464	64.67
TCE	Blank	−1567	2.50	510	474	−	−1594	3.26	485	472	−
	0.05	−1556	1.21	481	484	51.63	−1593	1.32	484	492	59.60
	0.1	−1554	1.04	458	497	58.31	−1590	1.13	486	477	65.33
	0.2	−1553	0.93	460	470	62.76	−1593	1.00	485	469	69.33
	0.3	−1555	0.83	476	503	66.84	−1586	0.84	496	459	74.33
	0.4	−1549	0.69	470	485	72.51	−1593	0.70	492	455	78.53
CSE	Blank	−1567	2.50	510	474	−	−1563	3.26	485	472	−
	0.1	−1554	1.75	470	508	31.59	−1604	2.02	471	515	37.91
	0.2	−1544	1.53	470	488	40.87	−1581	1.75	470	499	46.33
	0.3	−1505	1.39	389	512	46.75	−1600	1.54	392	522	52.81
	0.4	−1503	1.08	440	531	59.76	−1566	1.14	452	496	65.01
	0.5	−1501	0.89	457	503	65.05	−1586	0.84	475	494	74.11

Table 4: Activation parameters for the corrosion of aluminum and 6063 aluminum alloy in 0.5 M sodium hydroxide containing different concentrations of inhibitors

Inhibitors	Conc. of inhibitors (g L^{-1})	Aluminum			6063 Aluminum alloy		
		E_a (kJ mol^{-1})	$\Delta H^{\#}$ (kJ mol^{-1})	$\Delta S^{\#}$ (J mol^{-1} K^{-1})	E_a (kJ mol^{-1})	$\Delta H^{\#}$ (kJ mol^{-1})	$\Delta S^{\#}$ (J mol^{-1} K^{-1})
GIE	0.0	23.66	21.66	−147.58	21.61	19.05	−148.69
	0.05	11.30	8.69	−192.56	6.96	9.57	−214.05
	0.1	7.52	4.91	−205.44	4.75	7.36	−223.78
	0.2	7.10	4.49	−207.63	4.51	3.11	−232.09
	0.3	5.46	2.85	−213.84	1.82	1.90	−246.98
	0.4	0.42	1.29	−233.80	0.50	0.78	−255.46
TCE	0.0	23.66	21.66	−147.58	21.61	19.05	−148.69
	0.05	36.24	33.63	−112.60	34.97	32.36	−116.18
	0.1	39.87	37.26	−101.75	37.26	34.65	−109.94
	0.2	40.24	37.64	−101.20	39.29	36.68	−104.29
	0.3	41.64	39.03	−97.64	42.78	40.17	−94.32
	0.4	46.80	44.19	−82.22	44.33	41.72	−90.62
CSE	0.0	23.66	21.66	−147.58	21.61	19.05	−148.69
	0.1	32.88	30.28	−120.34	31.82	29.21	−123.06
	0.2	33.80	31.19	−118.45	33.36	30.75	−119.18
	0.3	35.44	32.84	−113.90	34.54	31.93	−116.38
	0.4	39.52	37.16	−101.61	37.23	34.63	−110.02
	0.5	39.77	36.92	−104.11	44.78	42.17	−87.71

Table 5: Thermodynamic parameters for the adsorption of inhibitors on aluminum and 6063 aluminum alloy in 0.5 M sodium hydroxide at different temperatures

Inhibitors	Temp (K)	Aluminum			6063 Aluminum alloy		
		ΔG^{o}_{ads} (kJ mol^{-1})	ΔH^{o}_{ads} (kJ mol^{-1})	ΔS^{o}_{ads} (J mol^{-1} K^{-1})	ΔG^{o}_{ads} (kJ mol^{-1})	ΔH^{o}_{ads} (kJ mol^{-1})	ΔS^{o}_{ads} (J mol^{-1} K^{-1})
GIE	303	−15.77	23.55	−129.66	−17.60	23.92	−136.87
	308	−16.30			−18.10		
	313	−17.11			−19.02		
	318	−17.61			−19.54		
	323	−18.36			−20.30		
TCE	303	−16.31	−25.11	−28.87	−18.81	−25.16	−20.95
	308	−16.25			−18.74		
	313	−16.15			−18.66		
	318	−16.06			−18.51		
	323	−15.98			−18.39		
CSE	303	−13.33	−50.34	−121.91	−14.06	−51.76	−124.18
	308	−12.81			−13.47		
	313	−12.23			−13.04		
	318	−11.71			−12.45		
	323	−10.84			−11.46		

Table 6: Optimum efficiency by the PDP method for the corrosion of aluminum and 6063 aluminum alloy in sodium hydroxide containing different concentrations of GIE, TCE and CSE

Inhibitor	Temp (℃)	[NaOH]	Conc. of Inhibitor (g L^{-1})	*IE* (%)	
				Aluminum	6063 Al alloy
GIE	50	0.5	0.4	75.76	81.87
		1.0	0.5	71.39	77.82
		2.0	0.6	66.19	73.08
TCE	30	0.5	0.4	72.51	78.53
		1.0	0.5	68.05	74.37
		2.0	0.6	62.87	69.64
CSE	30	0.5	0.5	65.05	74.11
		1.0	0.6	62.48	67.12
		2.0	0.7	55.94	62.59

Table 7: Comparison of inhibition efficiencies of GIE, TCE and CSE (0.4 g L^{-1}) by PDP method for the corrosion of aluminum and 6063 aluminum alloy in 0.5 M sodium hydroxide

Inhibitor	Temp (℃)	Metal	[NaOH]		
			0.5 M	1.0 M	2.0 M
GIE	50	Aluminum	75.76	65.72	56.44
		6063 Al alloy	81.87	73.62	63.88
TCE	30	Aluminum	72.51	68.05	62.87
		6063 Al alloy	78.53	74.37	69.64
CSE	30	Aluminun	65.05	62.48	55.94
		6063 Al alloy	74.11	67.12	62.59

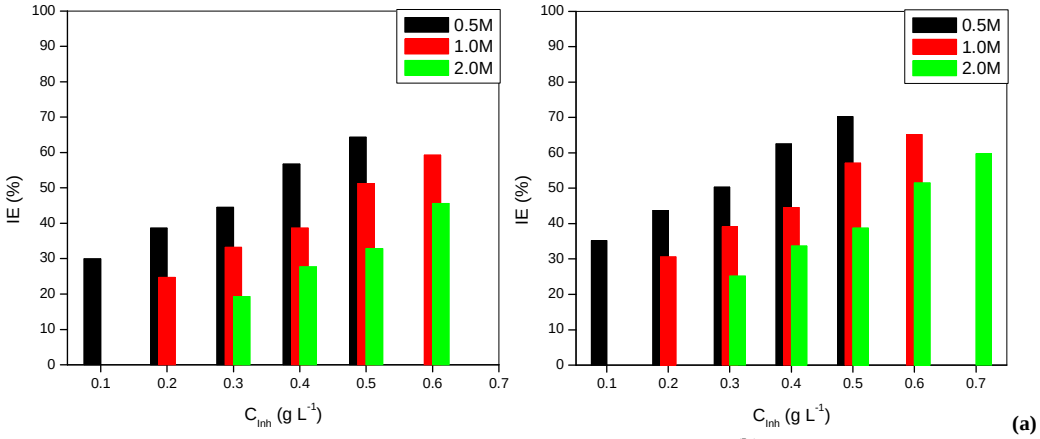

Figure 1: The variation of inhibition efficiency containing different concentrations of TCE in sodium hydroxide for the corrosion of (a) aluminum; (b) 6063 aluminum alloy at 30 ℃

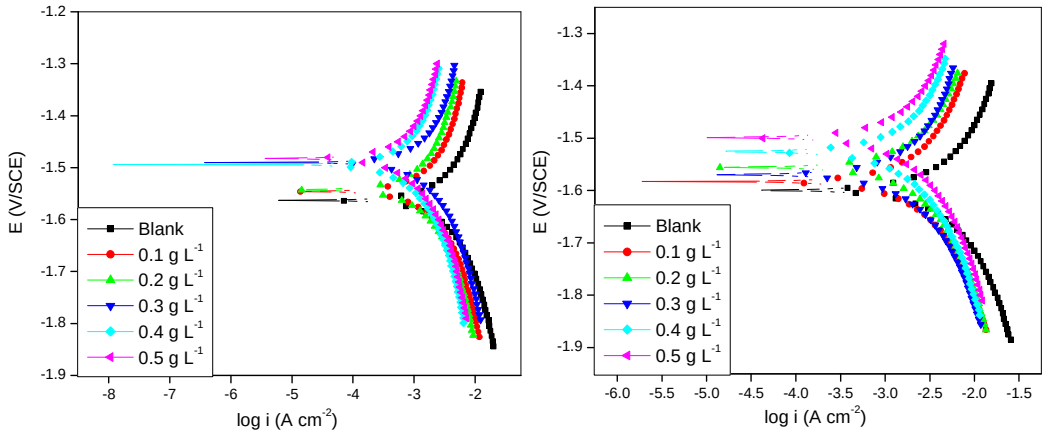

Figure 2: Potentiodynamic polarization plots in 0.5 M sodium hydroxide containing different concentrations of CSEat 30 ℃ for the corrosion of (a) aluminum; (b) 6063 aluminum alloy

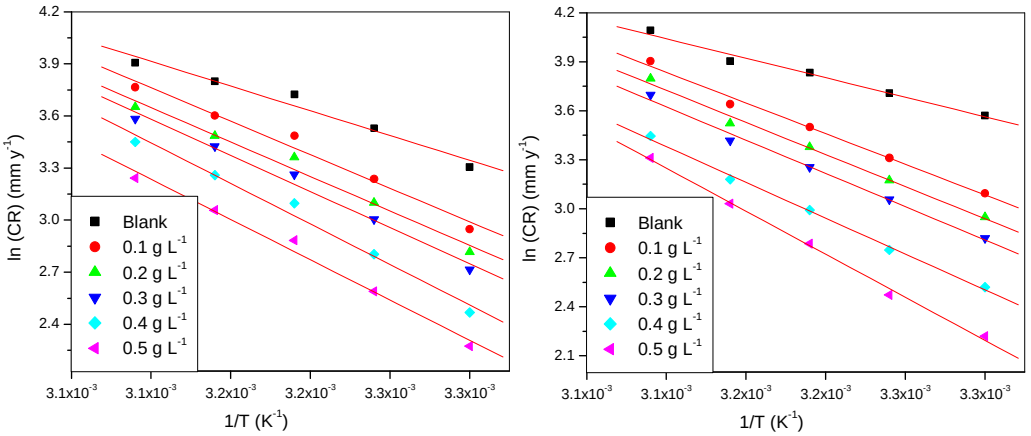

Figure 3: Arrhenius plots in 0.5 M sodium hydroxide containing different concentrations of CSE for the corrosion of (a) aluminum; (b) 6063 aluminum alloy

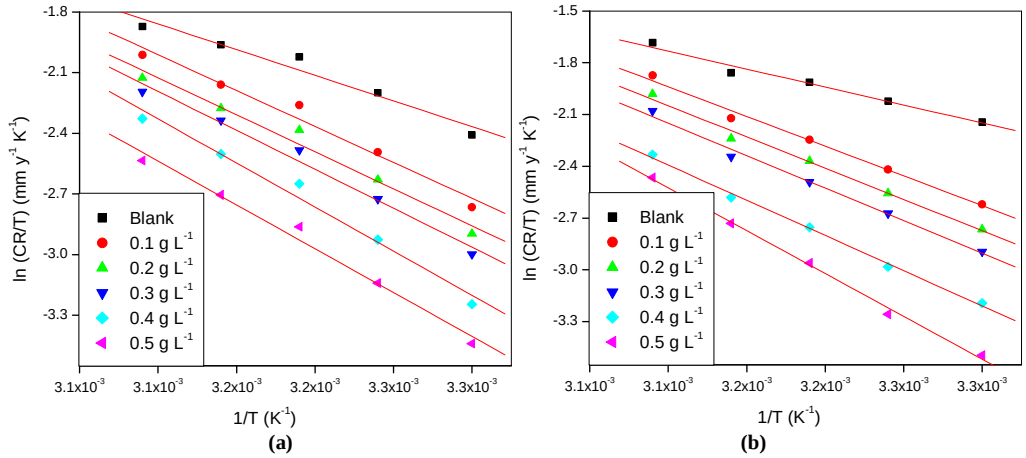

Figure 4: Plots of ln (*CR/T*) versus *1/T* in 0.5 M sodium hydroxide containing different concentrations of CSE for the corrosion of (a) aluminum; (b) 6063 aluminum alloy

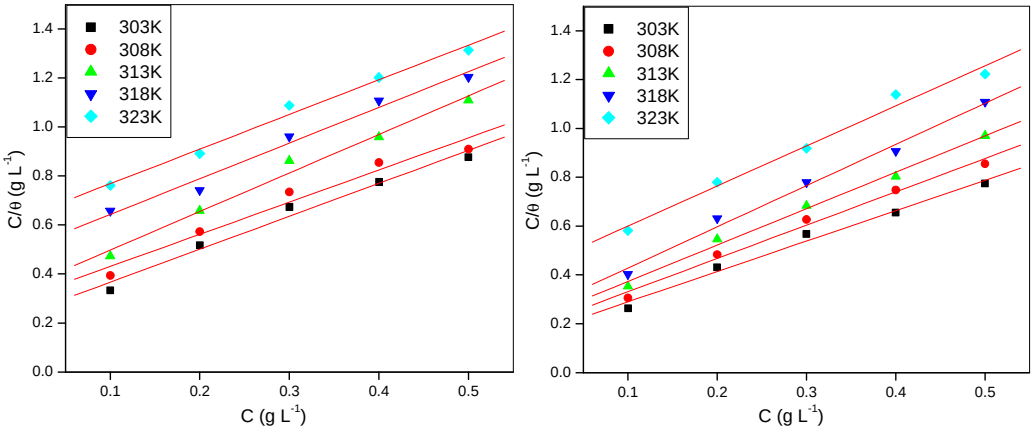

Figure 5: Langmuir adsorption isotherms for the adsorption of CSE in 0.5 M sodium hydroxideat different temperatures for the corrosion of (a) aluminum; (b) 6063 aluminum alloy

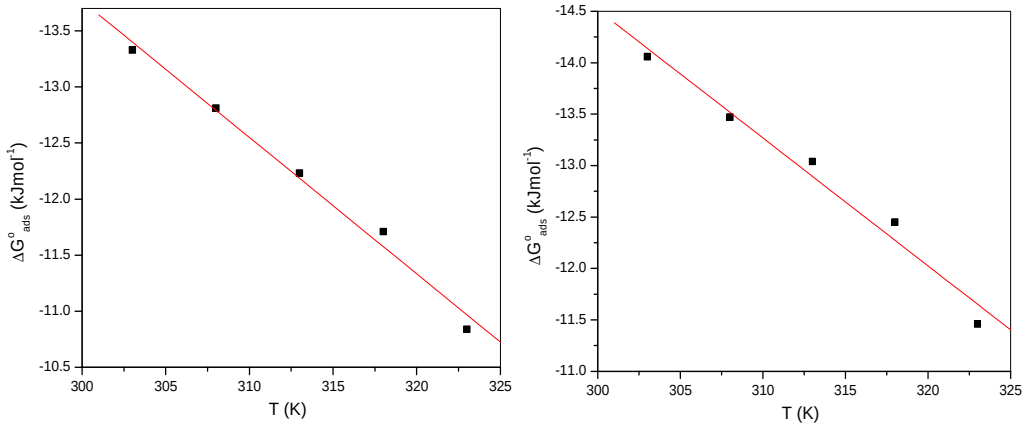

(a) **(b)**

Figure 6: Plot of free energy of adsorption versus temperature for the adsorption of CSEin 0.5 M sodium hydroxide for the corrosion of(a) aluminum; (b) 6063 aluminum alloy

3.7Comparison of percentage inhibition efficiencies of GIE, TCE and CSE in sodium hydroxide medium

Studies were done by adding different concentrations of the inhibitor to the system to get maximum efficiency. Among the three studied inhibitors, GIE underwent chemisorption by forming the co-ordinate bond with the metal by sharing the electron pair of heteroatom. The maximum efficiency of 75.76 % was obtained for the addition of 0.4 g L^{-1} of the inhibitor at 50 ℃ for aluminum (Table 7). The maximum inhibition efficiency of 81.87 % was obtained for the addition of 0.4 g L^{-1} of the inhibitor at 50 ℃ 6063 aluminum alloy.

Corrosion inhibition behavior of TCE and CSE were almost the same. Both of them underwent physical adsorption. TCS acted predominately as mixed inhibitor, with more control over anodic reaction. CSE acted as anodic inhibitor. For a given concentration of the inhibitor (0.4 g L^{-1}), the inhibition efficiency was more for TCE, at all studied concentrations of sodium hydroxide. This is mainly attributed to the larger molecular size of the principal constituents of TCE. The TCE molecules contain a large number of –OH groups due to these they have higher efficiency than CSE. However it must be noted that, for a given concentration of the inhibitor, all of them showed the inhibition efficiency of more than 60 %.

CONCLUSION

- The inhibition efficiency of the GIE increased with increase in the concentration of the inhibitor and increased with increase in temperature.
- The inhibition efficiencies of TCE and CSE increased with increase in the concentrations of the inhibitors and decreased with increase in temperature.
- Adsorption of GIE on the metal surface was through chemisorption, whereas adsorption of TCE and CSE were through physisorption.
- The inhibition efficiencies of GIE, TCE and CSE were higher for 6063 aluminum alloy than for aluminum.
- The inhibition efficiencies of GIE, TCE and CSE decreased with increase in concentrations of sodium hydroxide.
- Results obtained by the weight loss method and potentiodynamic polarization were in good agreement with one another.
- GIE, TCE and CSE are good inhibitors for the corrosion control of aluminum and 6063 aluminum alloy in sodium hydroxide medium.

REFERENCES

[1] C. Vargel, *Corrosion of Aluminium*: Elsevier, **2004**.
[2] Ambrish Singh, Eno E. Ebenso, and M. A. Quraishi, *International Journal of Corrosion*, **2012**, 2012: 1-20.
[3] S. Ramananda, S. Vivek, and S. Gurmeet, *Portugaliae Electrochimica Acta*, **2011**, 29: 405-417.
[4] S. Padhye, A. Ahmad, N. Oswal, and F. Sarkar, *Journal of Hematology & Oncology*, **2009**, 2: 1-13.
[5] N. N. Barthakur and N. P. Arnold, *Food Chemistry*, **1991**, 40: 213-219.
[6] C. L. Chang and C. S. Lin, *Evidence-Based Complementary and Alternative Medicine*, **2012**.

[7] Farooq Anwar, Muhammad Sulman, Abdullah Ijaz Hussain, Nazamid Saari, Shahid Iqbal, and U. Rashid, *Journal of Medicinal Plants Research*, **2011**, 5: 3537-3544.
[8] I. B. Md. Nazrul, B. Jaripa, and S. Mahbuba, *Bangladesh J Pharmacol*, **2009**, 4: 150-153.
[9] S. S. Handa, S. P. S. Khanuja, G. Longo, and D. D. Rakesh, *Extraction Technologies for Medicinal and Aromatic Plants*: Earth, Environmental and Marine Sciences and Technologies, **2008**.
[10] M. G. Fontana, *Corrosion Engineering*: Tata McGraw-Hill, **2005**.
[11] E. McCafferty, *Introduction to Corrosion Science*: Springer, **2010**.
[12] L. I. Antropov, *Corrosion Science*, **1967**, 7: 607-620.
[13] I. L. Rozenfel′d, *Corrosion Inhibitors*: McGraw-Hill, New York, **1981**.
[14] N. Dinodi and A. N. Shetty, *Corrosion Science*, **2014**, 85: 411-427.
[15] S. M. A. Shibli and V. S. Saji, *Corrosion Science*, **2005**, 47: 2213-2224.
[16] S. K. Milonjic, *J. Serb. Chem. Soc.*, **2007**, 72: 1363–1367.
[17] ASTM Standard G 102 – 89, "Standard Practice for Calculation of Corrosion Rates and Related Information from Electrochemical Measurements," *ASTM International, West Conshohocken, PA*, **2010**.
[18] B. S. Sanatkumar, J. Nayak, and A. Nityananda Shetty, *Journal of Coatings Technology and Research*, **2012**, 9: 483-493.
[19] X. Li and S. Deng, *Corrosion Science*, **2012**, 65: 299-308.
[20] X. Li, S. Deng, and H. Fu, *Corrosion Science*, **2011**, 53: 2748-2753.
[21] B. S. Sanatkumar, J. Nayak, and A. Nityananda Shetty, *International Journal of Hydrogen Energy*, **2012**, 37: 9431-9442.
[22] F. Bentiss, M. Lebrini, and M. Lagrenée, *Corrosion Science*, **2005**, 47: 2915-2931.
[23] M. A. Hegazy and M. F. Zaky, *Corrosion Science*, **2010**, 52: 1333-1341.
[24] M. A. Amin, M. A. Ahmed, H. A. Arida, T. Arslan, M. Saracoglu, and F. Kandemirli, *Corrosion Science*, **2011**, 53: 540-548,.
[25] S. Deng and X. Li, *Corrosion Science*, **2012**,64: 253-262.
[26] G. K. Gomma and M. H. Wahdan, *Materials Chemistry and Physics*, **1995**, 39: 209-213.
[27] S. Martinez and I. Stern, *Applied Surface Science*, **2002**, 199: 83-89.
[28] A. S. Fouda, A. A. Al-Sarawy, F. S. Ahmed, and H. M. El-Abbasy, *Corrosion Science*, **2009**, 51: 485-492.
[29] P. D. R. Kumari, J. Nayak, and A. N. Shetty, *Journal of Coatings Technology and Research*, **2011**, 8: 685-695.
[30] L. Tang, G. Mu, and G. Liu, *Corrosion Science*, **2003**, 45: 2251-2262.
[31] M. A. Hegazy, H. M. Ahmed, and A. S. El-Tabei, *Corrosion Science*, **2011**, 53: 671-678.
[32] S. T. Arab, *Materials Research Bulletin*, 43: 510-521, **2008**.
[33] S.-I. Pyun and S.-M. Moon, *Journal of Solid State Electrochemistry*, **2000**, 4: 267-272.
[34] A. J. Brock and G. C. Wood, *Electrochimica Acta*, **1967**, 12: 395-412.
[35] I. B. Obot and N. O. Obi-Egbedi, *Colloids and Surfaces A: Physicochemical and Engineering Aspects*, **2008**, 330: 207-212.
[36] H. Hohl and W. Stumm, *Journal of Colloid and Interface Science*, **1976**, 55: 281-288.
[37] M. A. Amin, Q. Mohsen, and O. A. Hazzazi, *Materials Chemistry and Physics*, **2009**, 114: 908-914.
[38] O. K. Abiola and J. O. E. Otaigbe, *Corrosion Science*, **2009**, 51: 2790-2793.
[39] M. Miadoková and J. Petrtýlová, *Chem. Paper*, **1985**, 39: 237-244.
[40] A. Singh, V. K. Singh, and M. A. Quraishi, *International Journal of Corrosion*, vol. **2010**, 2010:doi:10.1155/2010/275983.